

Chapter 4

Simulations of Tests of Polymeric Composites Based on Experimental Data



Jan Krmela, Vladimíra Krmelová, Artem Artyukhov, Cornelia Lex,
and Darina Ondrušová

4.1 Introduction

It is necessary to have knowledge about geometry, material parameters, cross-section, and structure of a tire casing (number of layers of a belt and carcass, information about a bead and cap ply) and other parameters for creations of computational models of a tire casings as polymeric composites for the strain–stress analysis of a tire under the vertical load, modal analysis etc. Tire casings have different constructions depending on the type of transport means. The construction of tires is different for passenger cars, trucks, off-highway cars and sport cars. A standard automobile radial tire casing consists of elastomer parts and parts with textile-cords and steel-cords in a tire tread as reinforcements (Krmela 2017). The structure parts applied into passenger car radial tire casings are textile carcass plies, a textile cap ply (called an overlap belt) and steel-cord belts. These structures of a tire have a different cord material, cord

J. Krmela (✉) · V. Krmelová · D. Ondrušová
Faculty of Industrial Technologies in Púchov, Alexander Dubček University of Trenčín, Ivana
Krasku 491/30, 020 01 Púchov, Slovak Republic
e-mail: jan.krmela@tuni.sk

V. Krmelová
e-mail: vladimira.krmelova@tuni.sk

D. Ondrušová
e-mail: darina.ondrusova@tuni.sk

A. Artyukhov
Sumy State University, Academic and Research Institute of Business, Economics and
Management, Sumy State University, 2, Rymaskogo-Korsakova St, Sumy 40007, Ukraine
e-mail: a.artyukhov@pohnp.sumdu.edu.ua

C. Lex
Mechanical Engineering and Economic Sciences, Technical University of Graz, Inffeldgasse
11/II, 8010 Graz, Austria
e-mail: cornelia.lex@tugraz.at

angle (e.g., for a steel belt there is applied an angle of 21–33° in a radial tire casing for a passenger car), the construction of cord and number of layers (single-layer or multi-layer). Therefore, tires have specific deformation properties. Data about cross-sections, construction-reinforcing plies, etc. are a necessary input for the creation of computational models of tires. The image analysis is applied for obtaining the information about geometric parameters of cords such as distances between cords and EPM (EPM is density—a number of ends (filaments) per one meter of width of layer), ply thickness, cord diameters, etc. The steel-cord of typical tire casings has the construction of $2 + 2 \times 0.28$ mm (the cord consists of four filaments) or 2×0.30 mm (two filaments). The steel-cord belt consists of two symmetrical layers. The geometric parameters, which are obtained by an image analysis of the cross-section, will be used as necessary geometric input data in order to create a computational model with a real configuration of cords.

For example, the simulation of tensile testing of composite is described in (Nirbhay et al. 2014), in which the authors used the FEM software Abaqus. In the case of cyclic loading of composites and computational simulations of these tests (Muc 2000; Krmela 2021), which is a more specific area, many simplifying assumptions are used with can lead to inaccurate results. In this article, the authors used FEA (Finite Element Method) software ANSYS Mechanical for the computational simulation of composites. The APDL (Ansys Parametric Design Language) in ANSYS is used for created of 3D computational models.

For the description of rubber matrix of composites, several material constitutive models have been considered in existing works to capture the hyperelasticity of elastomers for determination of material parameters, based on the tensile test or Shore A hardness (Krmela et al. 2021) for elastomer specimens for example. Among these the Mooney-Rivlin model (Krmela et al. 2021) is the most used for computational modelling of tires. It shows satisfactory results for the range of elongation (strain) up to 150%. There exists a large family of Mooney-Rivlin material models developed for a pool of hyperelastic materials. In the scope of this article and for the description of the behaviour of elastomers in tire casings, the Mooney-Rivlin material model used is the one with two parameters, which is sufficient to cover the range of strain abovementioned.

4.2 Materials and Methods and Computational Models

4.2.1 Materials Used

The PA 66 and PES textile fibres are used for passenger tires especially for common purposes. The sidewall also shows the material of cords and number of plies in the sidewall and under the tread of tire casing. The tire with symbol Extra load may have two polyester or two polyamide plies. The textile carcass EPM is from 700 to 1150 m⁻¹. The EPM of textile cap ply is 1100–1200 m⁻¹. For computational

modelling the elastic modulus of elasticity and Poisson ratio are used as material input parameters of textile reinforcements. From producer of textile cord the LASE modulus is used. LASE is modulus of elasticity for elongation 5% (LASE is acronym from Load At Specific Elongation 5%). Other way is determination of modulus as stress necessary on elongation 100% obtained by extrapolation for elongation 2%. In this article, the PA 66 is used as textile cords. Statical tensile modulus of elasticity of PA 66 (Shiguo 2004) is from 900 to 3450 MPa or from 9 to 50 cN/dtex. Typically values of moduli of elasticity are in Table 4.1. Usually, the experimental conditions are temperature 20 ± 2 °C, humidity $65 \pm 5\%$ and initial length between clamps of test machine (gauge length) 500 mm based on standard (ISO 2062:2009). For the simulations, the modulus values of 3400 MPa and the Poisson ratio of 0.4 are entered. The two cord diameters are used for simulation, 0.4 mm for shear test simulation and 0.5 mm for tensile test simulation. The first variant of computational model with 0.4 mm cord diameter is intended for verification of the reinforcement modelling method based on shear test simulation. The second variant of computational model with 0.5 mm cord diameter is given by real data from tensile experiments.

The composite consists of a rubber matrix (elastomer drift for a textile cap is taken to produce the composite samples as matrix) with modulus of elasticity of 3.96 MPa. For the description of matrix is used the hyperelastic Mooney-Rivlin model, which is described by the two Mooney-Rivlin parameters. To determine the basic Mooney-Rivlin parameters, it is necessary to carry out the tensile test for elastomer specimens. The values of the Mooney-Rivlin parameters of elastomer parts and elastomer matrix (drift) are depicted in Table 4.2 for the Matador 165/65 R13 tire casing as a sample of the results.

The Mooney-Rivlin (MR) parameters obtained by the tests are 0.548 MPa (as C10 in ANSYS) and 0.112 MPa (as C01 in ANSYS) and incompressibility parameter d is 0.056 MPa^{-1} .

The geometrical parameters of specimens for tests are the specimen's length of 140 mm, width of 35 mm, initial length between the clamps of test machine is 100 mm, specimen's thickness is 1.1 mm and cord angle is 45° . The EPM is 870 m^{-1} . The

Table 4.1 Moduli of elasticity of textile cords

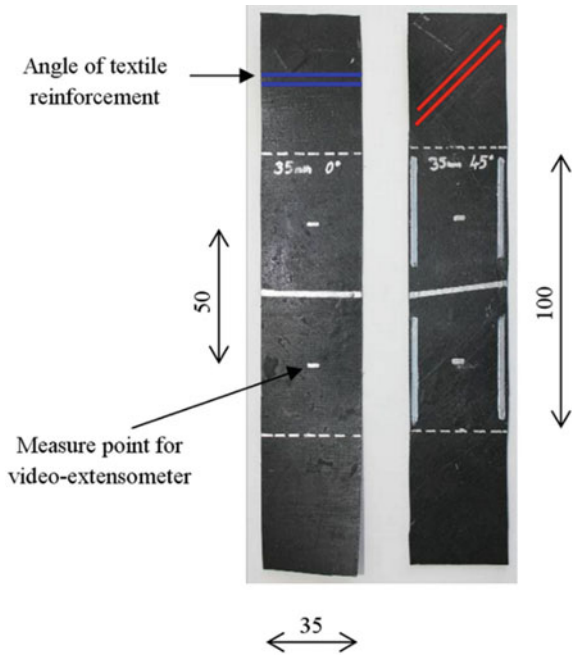
Mooney-Rivlin parameters	C10 [MPa]	C01 [MPa]	d [MPa ⁻¹]
Tread	0.417	0.519	0.103
Inner liner	0.109	0.259	0.206
Bead elastomer	0.692	0.371	0.267
Sidewall with a tread side edge	0.532	0.065	0.138
Bead bundle	-0.111	1.945	0.088
Elastomer drift for a steel-cord belt	0.638	0.284	0.151
Elastomer drift for a textile cap	0.548	0.112	0.056
Elastomer drift for a textile carcass	0.328	0.119	0.101

Table 4.2 Mooney-Rivlin parameters for elastomer parts of the Matador 165/65 R13

Material	Labeling of construction [tex]	Modulus of elasticity [GPa]
Polyester (PES)	PES 110 × 1 × 2	4
Polyamide 66 (PA 66)	PA 66 94 × 1 × 2	3.4
Rayon (viscose)	VS 184 × 1 × 3	11
Aramid	Aramid 167 × 1 × 2	25

initial length between the two points for video-extensometer is 50 mm (Fig. 4.1). Other cord angles such as 0° and 60° were also used in tests. This article focuses on the 45° cord angle.

Fig. 4.1 Specimens with geometric parameters (in mm)



4.2.2 Methods Used

The test machine Autograph AG-X plus 5 kN—Shimadzu with video-extensometer for large strain as tensile tests of composite materials with elastomer and viscoelastic materials with test mode Control of the software Trapezium X is used for tests. Before the tests, calibration of the video-extensometer is required. For computational modelling, the program ANSYS Mechanical is used.

It is possible to rely on publications which deal with computational modelling of composites in tires Krmela and Krmelová, shear computational simulation (Kießling et al. 2016; Basri et al. 2021), and standard ASTM D5379 ASTM (2019) focused on shear composites testing for the application of test specimen geometry for polymers and Ansys tutorials for composites (Kanani 2021).

4.2.3 Computational Models for Shear Test Simulation

The purpose of the models is to verify which method of modelling the reinforcement is ideal and to compare the results with each other. The models are also used to verify the calculation settings for large deformations in terms of the convergence of the calculation.

The volume SOLID186 element type with the Mixed U/P (meant for a mixed variational formulation with two fields: the displacement U and hydraulic pressure P. Recalling that the second field is introduced in the formulation to enforce the incompressibility condition to the potential energy of the variational problem) setting is used for computational models with MR parameters. One layer had a length and a width of 20 mm. EPM is 420 m^{-1} based on real geometric parameters for Matador tire casing, Table 4.3. Therefore, the distance between each cord is 2.38 mm.

The APDL procedure includes parameterization with the following parameters:

```
*cset,1,3,Distance,'Distance between cord [mm] ',2.38 (based on EPM
value)
*cset,4,6,Diameter,'Cord diameter [mm] ',0.5
*cset,7,9,Thickness,'Thickness of layer [mm] ',1.1
*cset,10,12,Width,'Width of layer [mm] ',20
*cset,13,15,Lengh,'Lengh of layer [mm] ',20
*cset,16,18,Angle,'Cord angle [degree] ',0
*cset,19,21,E,'Modulus of elasticity of cord [GPa] ',3.4
*cset,22,24,PR,'Poisson ratio [-] ',0.4.
```

The APDL procedure includes the computation of rubber modulus based on MR parameters which can be entered directly or are determined based on data from a tensile test:

```
D = (2*(1-2*PR_E)) / (CONST1(1)*(5*PR_E-2)+CONST1(2)*(11*PR_E-5))
!parameter of incompressibility
TB,HYPE,2,1,2,MOON
TBDATA,,CONST1(1),CONST1(2),D,, !parameters are in MPa;
```

Table 4.3 Geometric and material parameters of composite parts of Matador 165/65 R13

Composite part	Steel-cord belt	Textile cap	Textile carcass
Material of cord	Steel HT	PA66	PES
Number of layers	2	1	1
Thickness of one layer [mm]	0.95	0.8	0.95
Diameter of cord [mm]	0.6	0.4	0.48
EPM [m^{-1}]	961	420	1 160
Spacing between cords [mm]	1.04	2.38	0.86
Modulus of elasticity [GPa]	190	3.4	4
Poisson's ratio [-]	0.3	0.4	0.4

$$E_E = 6 * (CONST1(1) + CONST1(2)) \text{ !modulus of elasticity}$$

$$G_E = 2 * (CONST1(1) + CONST1(2)) \text{ !shear modulus}$$

$$K_E = 2/D \text{ !volume modulus.}$$

The models consist of two plus two composite layers between three steel sheets. The models are reverse loaded, the displacement in the z -axis is defined and the summary reaction forces at the area of steel edges (using these edges, the specimen will be clamped in the jaws of the testing machine) are searched. The initial condition is 5 mm displacement of the middle steel sheet (Fig. 4.2). Solution control settings: calculated prestress is switched on, nonlinear geometric effects are in the on state, time at the end of load step is 5 as defined displacement, number of substeps is 20 (it means that the increment of every substep is 0.25 mm in the z -axis).

Material parameters are: The first model included hyperelastic MR model for matrix with two MR parameters for rubber matrix and linear isotropic material for PA 66 cords with modulus values of 3400 MPa and the Poisson ratio of 0.4.

The second model is based on the homogenization of the entire cord and rubber composite system expressed by the parameters of the linear orthotropic material: moduli of elasticity $E_x = 228$ MPa, $E_y = E_z = 4.24$ MPa and Poisson main ratios $PR_{xy} = 0.486$, $PR_{yz} = 0.581$, $PR_{xz} = 0.49$. Shear moduli $G_{xy} = G_{yz} = G_{xz} = 1.506$ MPa. These parameters are obtained based on freeware CADEC (Computer Aided Design Environment for Composites) (Barbero 2022) based on material parameters of cord and matrix.

The third model is a model with the concrete element SOLID65 with real constant 0.07 volume ratio of PA 66 cords. The linear isotropic material is used for PA 66

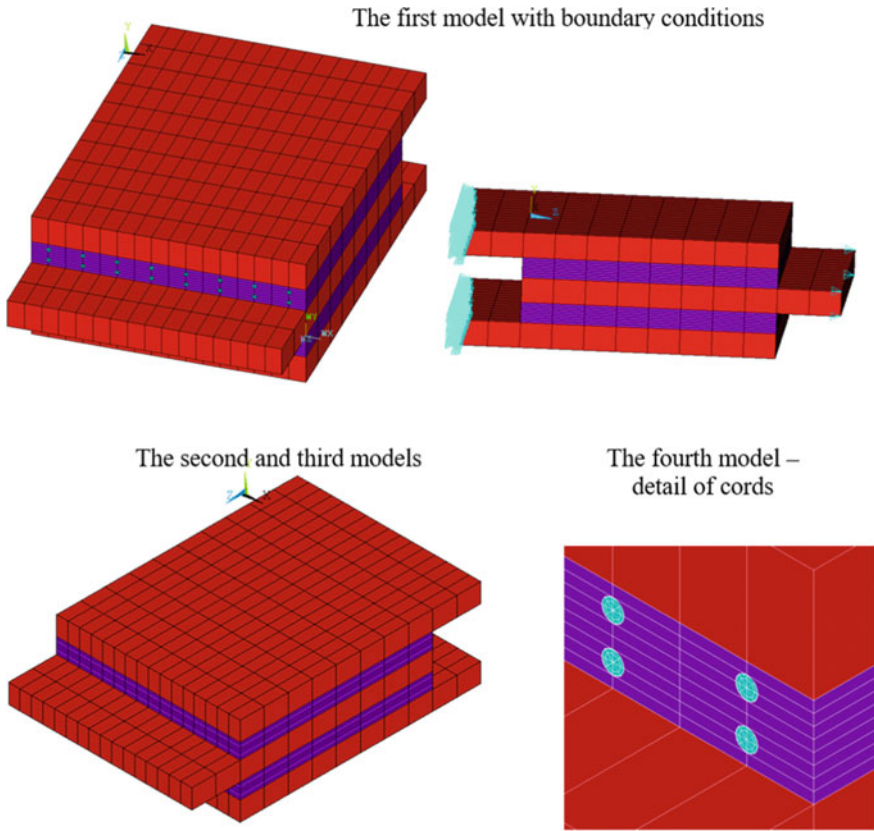


Fig. 4.2 Computational models for shear test simulation

cords with modulus values of 3400 MPa and the Poisson's ratio of 0.4 and for rubber matrix with modulus values of 3.96 MPa and the Poisson's ratio of 0.495.

The fourth model is a model with the element BEAM189 for PA 66 cord with beam section 0.2 mm of radius. The linear isotropic material is used for PA 66 cords and matrix such as 3rd model.

The computational models are presented in Fig. 4.2.

4.2.4 Computational Model for Tensile Test Simulation

The diameter of cords is 0.5 mm, EPM is 870 m^{-1} and thickness is 1.1 mm. The model consists of half of one layer with symmetry boundary conditions. The SOLID186 element type is used. The computational model consists of 22,836 elements and 106,053 nodes. The model has length 140 mm and the initial length between the

jaws of test machine 100 mm is modelling as remove of degrees of freedom in all axes (application of displacements on the selected nodes in areas of jaws). The model is reverse loaded, the displacement in x -axis is defined and reaction force at area of sliding clamp of test machine is searched. It is better for quickly convergence and speed solution. The initial condition is 30 mm displacement (this corresponds to an elongation (strain) of 30%). The solver PCG is used. The increment of every substep is 0.2 mm. A preload with a force of 2 N was considered, as in the experiment. A force of 2 N caused a deformation of 0.8 mm, similar to the case of the experiment.

The model included the hyperelastic MR model for the matrix with two MR parameters for rubber matrix ($C10 = 0.548$ MPa, $C01 = 0.112$ MPa and d is 0.056 MPa⁻¹ as was the case the first model for shear test simulation) and linear isotropic material for PA 66 cords with modulus values of 3400 MPa and the Poisson's ratio of 0.4. The elongation measurement points that represent the points for the video-extensometer are shown in the Fig. 4.3 with detail of the cross-section.

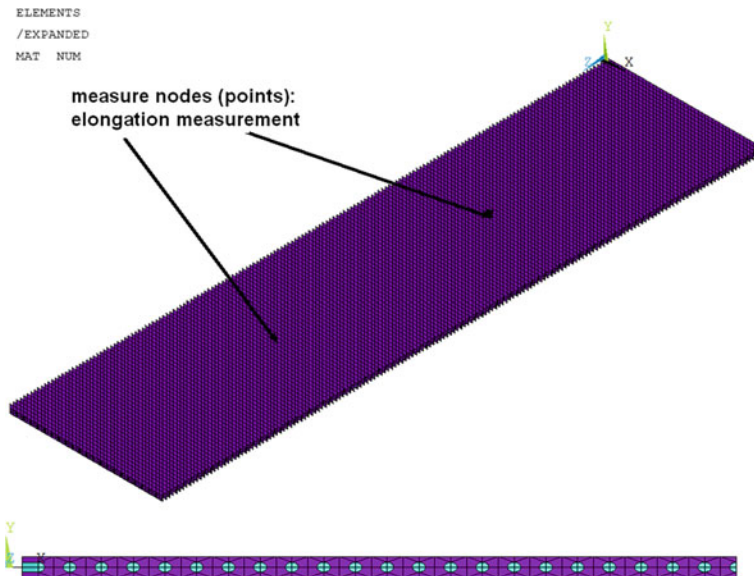


Fig. 4.3 Computational models for tensile test simulation with measurement points and detail of cross-section

4.3 Results and Discussion

4.3.1 Shear Test Simulations

The results from the computational modelling of strain–stress state of all variants are represented as the summary of displacement in Fig. 4.4. Reaction force–displacement dependences are shown in Fig. 4.5. The value of force in z -axis for deformation of 5 mm is 3243 N for the first model. The second model gives reaction forces in z -axis of 3452 N. The value of the third model is 2887 N. The resulting reaction force in z -axis for the fourth model is 3017 N. The rebar element (the fourth model) makes the model more flexible about 7% compared to the first model. If we were to compare the results for a half deformation of 2.5 mm, we would reach similar results in percentage.

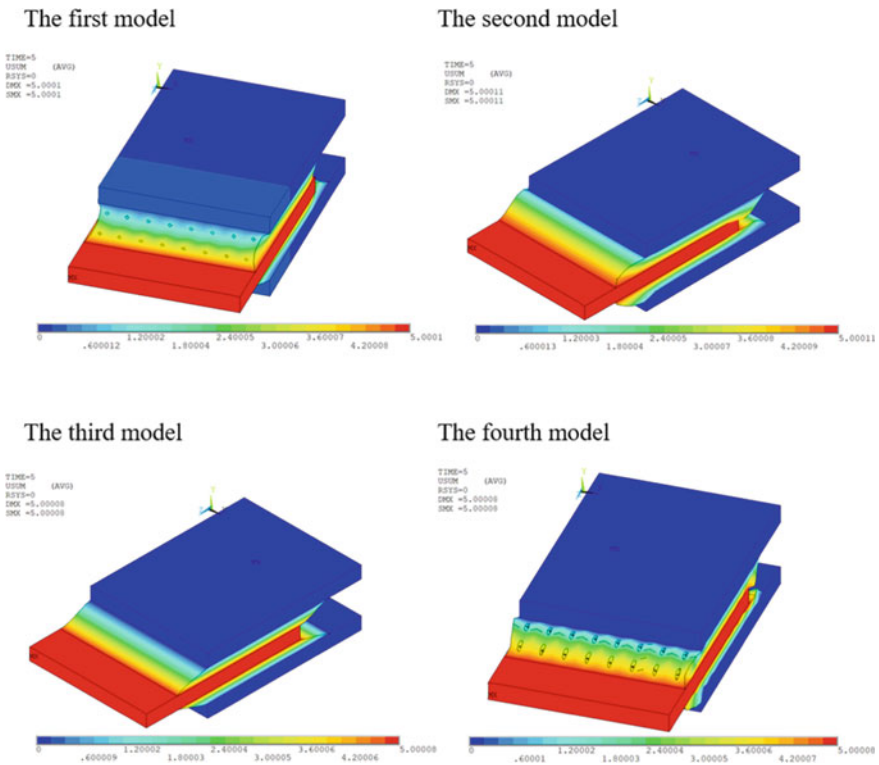
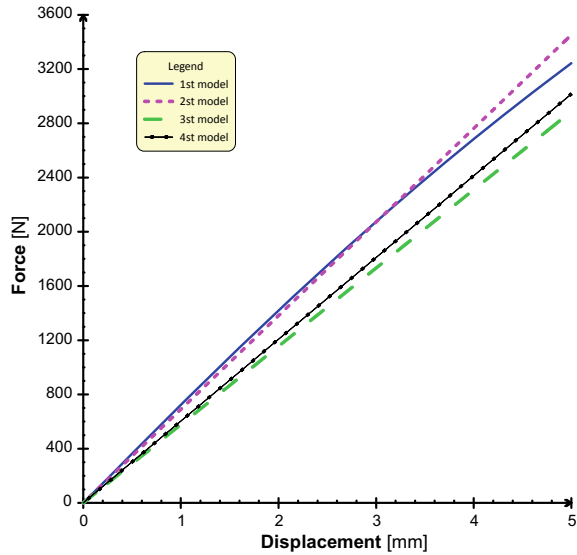


Fig. 4.4 Displacement from computational simulation of shear test

Fig. 4.5 Reaction force–displacement dependences from computational simulation of shear test



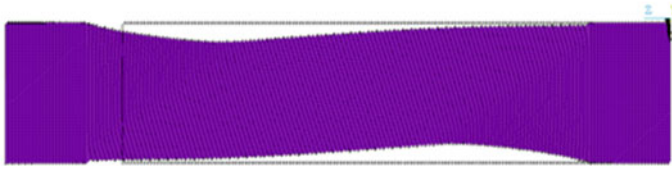
4.3.2 Tensile Test Simulation

The results from computational modelling as length displacement and width displacement for elongation 30% are in Figs. 4.6 and 4.7. The result as stress σ_1 (1st principal stress) in the PA 66 cords for elongation 30% is in Fig. 4.8. The value of reaction forces is 63.3 N. From experiment data, the tensile force 64.7 N causes an elongation of 30%. The computational model has good tensile stiffness because the forces are very similar. The force value differences are to 2.2%. A comparison of calculation results with experimental data in terms of dependences of force on elongation, stress on elongation (between jaws) and real stress on elongation between measuring points for the video-extensometer are shown in Figs. 4.9 and 4.10.

4.4 Conclusions

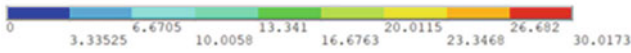
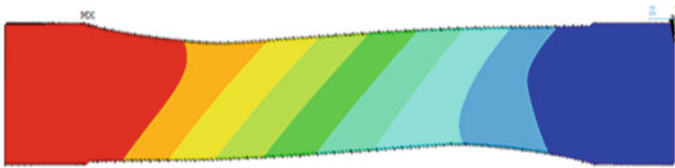
The different computational models with polymer cords were created. The simulations were created for different load states. The APDL procedure with parameterization of geometrical and material parameters such as cord distance and angle, thickness of the layer and number of layers for the creation of computational models was designed and programmed. The proposed APDL procedure is ready to create multi-layer models. The APDL procedure allows the user the choice of whether to use volume or beam elements to model cords and purpose of model—tensile or bend test simulations.

Deformation



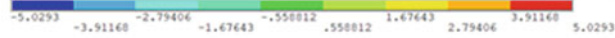
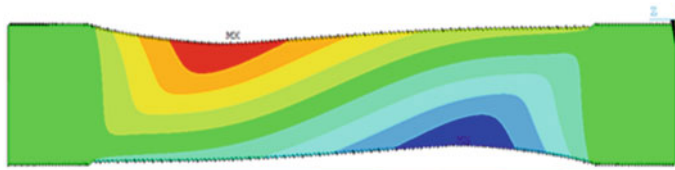
Summary displacement

USUM (AVG)
RSYS=0
DMX =30.0173
SMX =30.0173



Width displacement

UX (AVG)
RSYS=0
DMX =30.0173
SMN =-5.0293
SMX =5.0293



Length displacement

UZ (AVG)
RSYS=0
DMX =30.0173
SMN =-.01726
SMX =30.0173

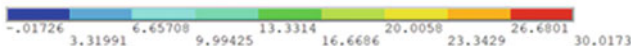
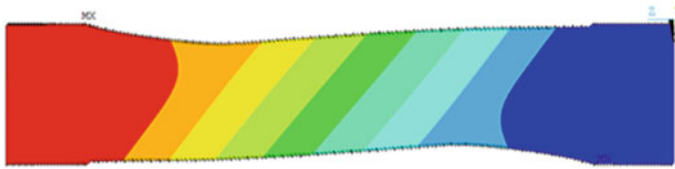
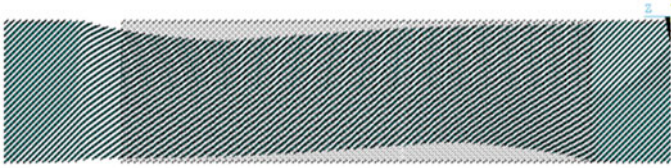


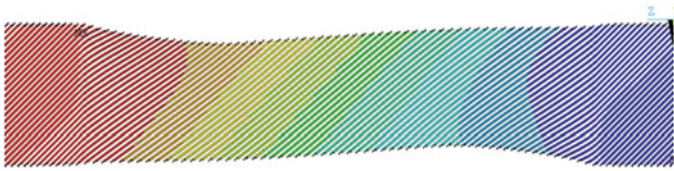
Fig. 4.6 Deformations and displacements from computational simulation of tensile test

Deformation



Summary displacement

USUM (AVG)
RSYS=0
DMX =30.0008
SMN =-.130E-08
SMX =30.0008



Width displacement

UX (AVG)
RSYS=0
DMX =30.0008
SMN =-5.0293
SMX =5.0293

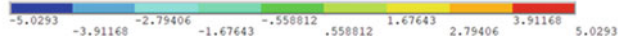
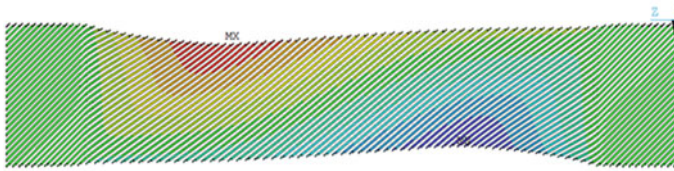


Fig. 4.7 Deformations and displacements of cords from computational simulation of tensile test

S1 (AVG)
DMX =30.0008
SMN =-10.5119
SMX =87.1584

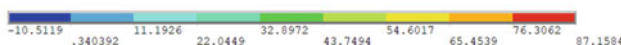
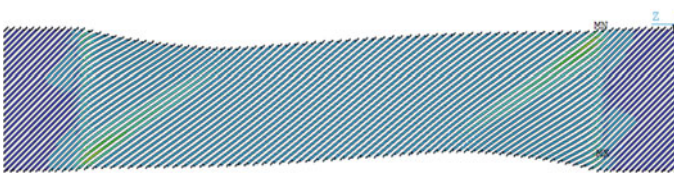
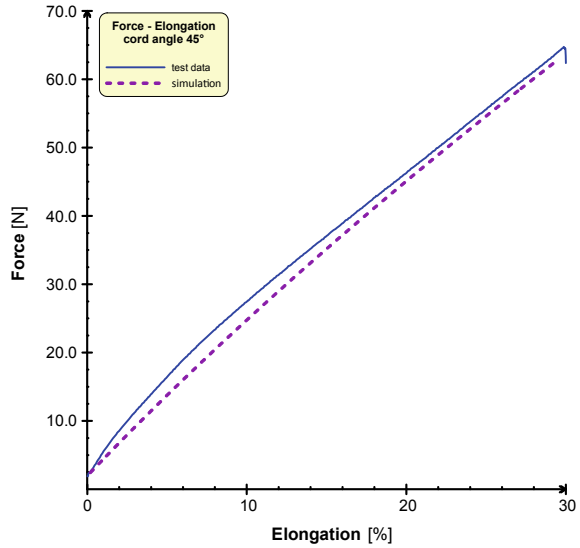


Fig. 4.8 Stress in the cords from computational simulation of tensile test

Fig. 4.9 Dependences of force on elongation



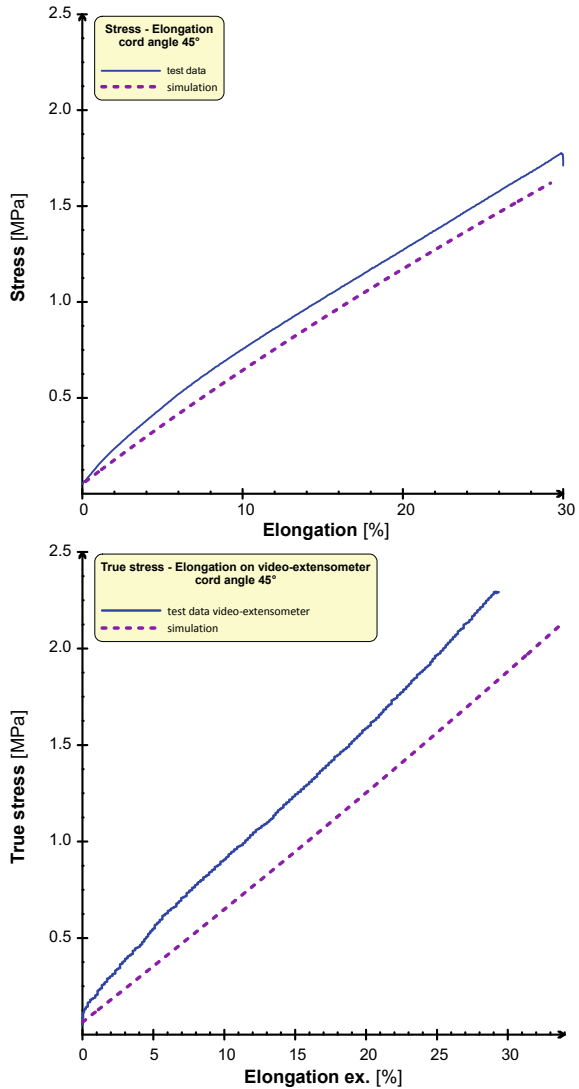
The results from tests and computational simulations of composites which represented parts of tire casings provide a better understanding of the mechanical properties of composites with textile reinforcements under static and specific loading.

Based on results, the best way is of reinforcement modelling is the first variant in which MR parameters for rubber matrix. The calculation time was a little longer than other models. The second way requires a good determination of material parameters. A slight change in the parameters of the moduli in tension and in shear can cause inaccurate results—there is a high sensitivity to the input material parameters.

The model for tensile test simulation gave quality results—force–elongation dependences almost overlap with an error of 5%. The model was prepared quickly by the APDL procedure, and the calculation setup guaranteed fast convergence.

Next, the simulations of multiaxial loading and the inclusion of the effect of temperature will be realized because these simulations are important for practice, as these calculations simulate to some extent the real states of loading and composites for engineering applications such as their use in vehicles not only in automobiles.

Fig. 4.10 Dependencies of stress on elongation (between jaws) and real stress on elongation between measuring points for the video-extensometer elongation



Acknowledgements This research work has been supported by the Operational Programme Integrated Infrastructure, co-financed by the European Regional Development Fund by the project: Advancement and support of R&D for "Centre for diagnostics and quality testing of materials" in the domains of the RIS3 SK specialization, Acronym: CEDITEK II., ITMS2014+ code 313011W442 and the Aktion Austria–Slovakia, project No. 2019-05-15-001 and the Cultural and Educational Grant Agency of the Slovak Republic (KEGA), project No. 003TnUAD-4/2022 "Simulations of basic and specific experiments of polymers and composites based on experimental data in order to create a virtual computational-experimental laboratory for mechanical testing".

References

- ASTM D5379/D5379M–19: Standard test method for shear properties of composite materials by the V-notched beam method
- Barbero EJ (2022) CADEC. <https://barbero.cadec-online.com/>. Accessed 1 July 2022
- Basri EI, Sultan MTH, Basri AA, Mustapha F, Ahmad KA (2021) Consideration of lamination structural analysis in a multi-layered composite and failure analysis on wing design application. *Materials* 14:3705
- ISO 2062:2009 Textiles—Yarns from packages—determination of single-end breaking force and elongation at break using constant rate of extension (CRE) tester
- Kanani AY (2021) Ansys tutorial for ACP (Full composite tutorial in ANSYS). https://www.researchgate.net/publication/332766462_Ansys_Tutorial_for_ACP_Full_composite_tutorial_in_ANSYS. Accessed 1 July 2022
- Kießling R et al (2016) On the development of an intrinsic hybrid composite. In: IOP Conference series: materials science and engineering, vol 118. pp 012017
- Krmela J (2017) Tire casings and their material characteristics for computational modeling. Oficyna wydawnicza słowarzyszenia menadżerów jakości i produkcji, Czestochowa
- Krmela J (2021) The influence of temperature and other parameters on the tensile properties of polymer composites and polymers under cyclic loading. Oficyna wydawnicza słowarzyszenia menadżerów jakości i produkcji, Czestochowa
- Krmela J, Artyukhov A, Krmelová V, Pozovnyi O (2021) Determination of material parameters of rubber and composites for computational modeling based on experiment data. *J Phys: Conf Ser* 1741:012047
- Krmela J, Krmelová V, Artyukhov A, Sadjiep S, Bakošová A (2021) Computational simulation of the shear test of a multi-layered long-fibre composite with a polymer matrix. In: IOP conference series: materials science engineering, vol 1199. pp 012075
- Krmela J, Krmelová V (2016) Replacement of belt structure for FEA of tire. *Proc Eng* 136:132–136
- Muc A (2000) Design of composite structures under cyclic loads. *Comput Struct* 76:211–218
- Nirbhay M, Dixit A, Misra RK, Singh Mali H (2014) Tensile test simulation of CFRP test specimen using finite elements. *Proc Mater Sci* 5:267–273
- Shiguo R et al (2004) Mechanical properties and failure behaviour of cord/rubber composites. *Appl Compos Mater* 11:353–357